International Journal of Biological Macromolecules 165 (2020) 472–482

Contents lists available at ScienceDirect

International Journal of Biological Macromolecules

journal homepage: http://www.elsevier.com/locate/ijbiomac

Design of a structure-based fluorescent biosensor from bioengineered arginine deiminase for rapid determination of L-arginine

Suet-Ying Tam [a,1], Sai-Fung Chung [a,1], Yu Wai Chen [a], Yik-Hing So [a], Pui-Kin So [a], Wing-Lam Cheong [b], Kwok-Yin Wong [a,*], Yun-Chung Leung [a,*]

[a] Department of Applied Biology and Chemical Technology, Lo Ka Chung Research Centre for Natural Anti-Cancer Drug Development and State Key Laboratory of Chemical Biology and Drug Discovery, The Hong Kong Polytechnic University, Hung Hom, Kowloon, Hong Kong, China
[b] Department of Science, School of Science and Technology, The Open University of Hong Kong, Hong Kong

ARTICLE INFO

Article history:
Received 10 July 2020
Received in revised form 7 September 2020
Accepted 18 September 2020
Available online 21 September 2020

Keywords:
L-arginine
Biosensor
Fluorescence

ABSTRACT

Rationally designed mutations on recombinant arginine deiminase (ADI) could act as a 'turn-off' L-arginine (L-Arg) fluorescent biosensor and provide an alternative method for rapid determination of L-Arg. Double mutations were introduced on the Cys^{251}→Ser^{251} and Thr^{265}→Cys^{265} of recombinant ADI, rendering a single cysteine present on the protein surface for the site-specific attachment of a fluorophore, fluorescein-5-maleimide. The double mutations on ADI (265C) and its fluorescein-labelled form (265Cf) conserved the catalytic efficiency of wild-type ADI. Upon binding to L-Arg, 265Cf induced structural conformational changes and rendered the fluorescein moiety to move closer to Trp^{264}, resulting in fluorescence quenching. The duration of fluorescence quenching was dependant on the L-Arg concentration. A linear relationship between the time at the maximum rate of fluorescence change and L-Arg concentrations, which ranged from 2.5 to 100 μM, was found with $R^2 = 0.9988$. The measurement time was within 0.15–4 min. Determination of L-Arg concentration in fetal bovine serum could be achieved by the standard addition method and without sample pre-treatment. The result showed a good agreement with the one determined by mass spectrometry, suggesting our biosensor as a promising tool for the detection of L-Arg in biological samples.

1. Introduction

L-Arginine (L-Arg) is recognized as one of the miracle molecules due to the significant roles it plays in acting as precursor and anti-aggregating agent of a lot of proteins and molecules for metabolism [1,2]. Its concentrations can be indicators of the degree of healthiness of people and the quality of food [3]. Generally, the normal L-Arg concentration in humans is about 100–120 μM [4]. This range can be a kind of references of physiological conditions since elevated plasma L-Arg concentration has been observed in some arginase deficiency persons while declined L-Arg concentration has been found in L-Arg auxotrophic cancer patients [3,5–12]. On the other hand, measurement of plasma L-Arg concentrations is one of the key parameters that reflects the potency of arginine-depleting drugs for the treatment of cancers [13–15]. In the area of food processing, L-Arg is an index for monitoring the safety of beverages, especially in wine production [16–19]. During the fermentation process, L-Arg is converted into urea, which is accumulated and sequentially reacts with ethanol to produce a hazardous and carcinogenic compound, ethyl carbamate [16–19]. Therefore, the monitoring of L-Arg concentrations in biological and food samples is fundamentally important.

There are numerous methods to detect L-Arg concentrations, such as ionization mass spectrometry and high-performance liquid chromatography to provide accurate quantitative analyses [20–22], but they involve high operating cost and long measurement time. Biosensors, on the contrary, can provide fast response and high specificity for determination, and thus, they are commonly used in drug discovery, diagnosis, and food safety and processing [23,24]. Different types of L-Arg biosensors have been developed and they exhibit wide linear detection ranges with rapid response time. Details of their characteristics are summarized in Table 1. However, these biosensors have the following drawbacks: (a) The specificity of biosensor is reduced due to using ammonium (NH_3) as an analyte. Additional measurement of NH_3 concentration is thus required for samples that contain NH_3 [25–27], (b) Two enzymes system (Arginase/Urease) might introduce more variations than one enzyme system into the detection of L-Arg [26,28–33].

Targeting the problems mentioned above, in the present study, we developed a fluorescent biosensor with a single enzyme, arginine deiminase (ADI), to directly measure L-Arg concentration. This enzyme

* Corresponding authors.
E-mail addresses: kwok-yin.wong@polyu.edu.hk (K.-Y. Wong), thomas.yun-chung.leung@polyu.edu.hk (Y.-C. Leung).
[1] These authors contributed equally to this work.

https://doi.org/10.1016/j.ijbiomac.2020.09.134

Table 1
Different types of L-arginine biosensors.

Analyte	Bio-receptor	Transducers	Working systems	Immobilization	Detection range (μM)	Response time (s)	Ref.
NH_3	Arg/Urs	Conductometric	Au coated ceramic plate	Cross-linking	100–1000	–	[28]
NH_3	Arg/Urs	Conductometric	Two Au-interdigitated film electrodes	Cross-linking	10–4000	120	[29]
NH_3	Arg/Urs	Potentiometric	Glass electrode	Cross-linking	25–310	600	[26]
NH_3	Arg/Urs	Amperometric	Three-electrode system	Electro- polymerization	70–600	10	[30]
NH_3	Arg/Urs	Fluorescent	O17-Ec membrane	Entrapment	100–10,000	~290	[31]
NH_3	Arg/Urs	Conductometric	Fused Al_2O_3 with Au interdigitated electrodes	Entrapment	2.5–500	20	[32]
NH_3	Arg/Urs	Amperometric	Three-electrode system	Electro-polymerization	150–600	60	[33]
NH_3	ADI	Amperometric	PANi composite screed-printed electrode	Cross linking	3–200	15	[25]
NH_3	ADI	Potentiometric	Nanocomposite file modified glassy carbon electrode	Cross linking	100–1000	10	[12]

Notes: Arg: Arginases; Urs: Ureases; ADI: arginine deiminase; O17-Ec: oxazine 170 perchlorate-ethyl cellulose; PANi: Polyanyline.

was bio-engineered for the site-specific attachment of the fluorophore, fluorescein-5-maleimide (F5M). The incorporation of F5M into ADI would allow the generation of fluorescence intensity changes upon the binding of L-Arg with ADI, showing a high specificity of the biosensor. Our biosensor could successfully detect the L-Arg concentration in fetal bovine serum, a result that was comparable with the results determined by Mass-spectrometry. Therefore, it provided an alternative method for rapid and accurate determination of L-Arg concentration in biological samples.

2. Materials and methods

2.1. Materials and instruments

The DNA sequence of wild-type arginine deiminase (WT-ADI) inserted into pET3a vector, pET3a/WT-ADI, was purchased from GeneScript. Fluorescein-5-maleimide (F5M) was purchased from Invitrogen. L-arginine (L-Arg) and fetal bovine serum (HyClone™) were purchased from ThermoFisher. Fluorescence measurements were performed on an Aglient Cary Eclipse Fluorescence Spectrophotometer (Agilent). Electrospray ionization mass spectrometry (ESI–MS) experiments were conducted using an Agilent 6540 QTOF mass spectrometer coupled with an Agilent 1290 Infinity UHPLC system.

2.2. Gene cloning and mutagenesis

Plasmid pET3a/WT-ADI was used as a template for site-directed mutagenesis according to the instruction of the QuikChange site-directed mutagenesis kit (Strategene). The codon for Cys^{251} residue was mutated to the codon for Ser^{251} using the following mutagenic primers. The mutated ADI was named as C251S.

Forward primer of C251S: 5′ GTTGCTAATAAAGAA***A***G***C***GAATTCAAA CGTATT 3′

Reverse primer of C251S: 5′ AATACGTTTGAATTC***GC******T***TTCTTTATTAG CAAC 3′

The plasmid pET3a/C251S was then used as a template for further site-directed mutagenesis to respectively generate two mutants by the following primers. They were named as 44C and 265C.

Forward primer of 44C:

5′ GACTATATTACACCAGCTAGACTAGATGAATTAT***GC***TTCTCAGCTAT CTTAGAA 3′

Reverse primer of 44C:

5′TTCTAAGATAGCTGAGAA***GC***ATTCATCTAGTCTAGCTGGTGTAATA TAGTC 3′

Forward primer of 265C:

5′ TGTTGCAATTAACGTTCCAAAATGG***TGC***AACTTAATGCA CTTAGA CACATG GC 3′

Reverse primer of 265C:

5′ GCCATGTGTCTAAGTGCATTAAGTT***GCA***CCATTTTGGAACGTTAATT GCAACA 3′

2.3. Expression and purification of ADI

Plasmids corresponding to WT-ADI and two mutants (44C and 265C) were transformed into BL21(DE3) for expression. A single colony was picked and grown overnight at 37 °C in sterile LB medium that contained 100 μg/ml ampicillin with shaking at 250 rev/min. The overnight culture was inoculated into 600 ml sterile LB medium with 100 μg/ml ampicillin in a ratio of 1:100 and grown at 37 °C with shaking at 250 rev/min for 2–3 h. When the culture optical density (OD_{600}) reached 0.6–0.8, one millimolar of IPTG was added for protein expression. The cell pellet was collected by centrifugation and lysed by an ultrasonic homogenizer (QSonica sonicators) in resuspension buffer (20 mM Tris buffer, pH 7.0). The crude cell lysates were centrifugated at 14,000 rpm for 2 h at 4 °C. The insoluble form was collected by centrifugation and resuspended in resuspension buffer for sonication. After that, it was collected by centrifugation at 14,000 rpm at 4 °C and washed by washing buffer twice (20 mM Tris, 1 mM EDTA, pH 7.0, and 4% Triton X-100). The resulting inclusion bodies were solubilized in a denaturing buffer (50 mM Tris, pH 8.5, 6 M guanidine-HCl, and 10 mM dithiothreitol) for 1 h at 37 °C. The solubilized proteins were refolded in a 100-fold excess volume of 20 mM Tris buffer, pH 7.0 at room temperature overnight. They were then purified by HiTrap Q HP (GE Healthcare). Target proteins were eluted at 20% of elution buffer (20 mM Tris, pH 7.0, 1 M NaCl) and analysed by sodium dodecyl sulfate polyacrylamide gel electrophoresis (SDS-PAGE).

2.4. Bicinchoninic acid (BCA) protein assay

Pierce™ BCA protein assay was used to determine the protein concentration following the manufacturer's instruction (Thermo Fisher Scientific).

2.5. Protein labelling

F5M was labelled as described with the following modifications. The ADI mutants were buffer exchanged into 20 mM Tris, pH 7.0. A 10 mM stock solution of F5M was prepared by dissolving it in dimethylformamide, and added to the ADI mutants in a molar ratio of 1:20. They were incubated in the dark for 2 h with shaking. After that, excess F5M was removed by dialysis with 20 mM Tris buffer using Amicon Ultra-15 (NMWL = 30, 000). The ADI mutants before and after labelling were analysed by SDS-PAGE.

2.6. Enzyme kinetics

The chromophore compound was detected at a wavelength of A_{530nm} in the presence of diacetyl monoxime, thiosemicarbazide, urea, and Fe^{3+} ions under 100 °C [34]. The amount of L-citrulline produced

by arginine deiminase per second was determined. Different concentrations of L-Arg solutions (200 μL) were pre-warmed at a 37 °C heat block. Reactions were performed by adding 5 μl of ADI (0.02 mg/mL) to specified concentration of L-Arg and terminated with 15 μl 80% trichloroacetic acid. The reaction time was 3 min. A colouring reagent was prepared by 1 volume of a mixture of solution A (80 mM diacetyl monoxime and 2.0 mM thiosemicarbazide) and 3 volumes of a mixture of solution B (3 M H_3PO_4, 6 M H_2SO_4, 2 mM $FeCl_3$). Eight hundred microliters of the colouring reagent were added to each reaction, and then the reaction mixtures were incubated at 100 °C for 10 min in the heat block. A_{530nm} was determined using ultraviolet-visible spectroscopy (Spectronic 20 Genesys Spectrometer).

2.7. Specific enzyme activity

The experimental procedure was the same as that of enzyme kinetics by using 20 mM L-Arg for the measurement. The specific activity of arginine deiminase enzyme was defined as the micromoles of L-citrulline formed per minute under given conditions per milligram proteins at 37 °C, pH 7.4 in phosphate buffered saline buffer (expressed in μmol min^{-1} mg^{-1}).

2.8. Mass spectrometry analysis

Liquid Chromatography-Electrospray Ionization Mass Spectrometry (LC-ESI-MS) experiments were performed with an Agilent 6540 QTOF mass spectrometer coupled with an Agilent 1290 Infinity UHPLC system. For the detection of intact proteins, samples were first injected into a C4 LC column and eluted with a linear gradient from 95% solvent A: 5% solvent B to 5% solvent A: 95% solvent B, where solvent A was 0.1% formic acid in MilliQ water and solvent B was acetonitrile with 0.1% formic acid. ESI-MS data were acquired with *m/z* range of 100–2500, from which multiply-charged mass spectra were obtained. The multiply charged mass spectra were deconvoluted by the MassHunter BioConfirm program (Agilent) to obtain the molecular mass of proteins. For the protein digestion experiment, proteins were first buffer exchanged into ammonium bicarbonate buffer and subsequently sequencing grade trypsin (Promega V5111) was added to the proteins in a ratio of trypsin:protein 1:50 (wt/wt). Protease digestions proceeded at 37 °C for 16 h. Peptides were separated and eluted in a C18 LC column with a linear gradient from 95% solvent A: 5% solvent B to 5% solvent A: 95% solvent B, where solvent A was 0.1% formic acid in MilliQ water and solvent B was acetonitrile with 0.1% formic acid. The ESI-MS was operated in auto-ms/ms mode for measurement of the molecular mass of peptides and their sequence-specific fragment ions resulted from collision-induced dissociation. Peptide assignment was performed with the Agilent Masshunter-BioConfirm software.

2.9. Florescence measurements

Different concentrations of L-Arg ranged from 2.5 to 100 μM, were prepared in PBS solution (pH 7.4). Four hundred and ninety-five microliters of each L-Arg solution was added in a quartz cuvette and mixed with 5 μl of 0.3 mg/ml of labelled ADI mutants. The real-time fluorescence intensity was recorded using an Aligent Cary Eclipse Fluorescence Spectrophotometer (Agilent). Both excitation and emission slit widths were 5 nm. The excitation wavelength was 494 nm while the emission wavelength was 518 nm.

2.10. Preparation of L-Arg spiked in serum and standard addition assay

Fetal bovine serum (Hyclone™) was used for L-Arg detection by our biosensor. It was four-folded diluted by PBS solution. Different concentrations of L-Arg ranging from 2.5 to 100 μM, were spiked into the diluted serum. Four hundred and ninety-five microliters of each L-Arg solution spiked in serum was added in a quartz cuvette and mixed with 5 μl of 0.3 mg/ml of 265Cf. Two different batches of 265Cf were used for the determination. The real-time fluorescence intensity was recorded using a Cary Eclipse Fluorescence Spectrophotometer (Agilent). Both excitation and emission slit widths were 5 nm. The excitation wavelength was 494 nm while the emission wavelength was 518 nm.

2.11. Molecular modelling

The substrate-bound model was created based on the crystal structure of arginine deiminase of *M. arginini* (WT-ADI) with Protein Data Bank Identifier (PDB ID) 1S9R [35]. The fluorophore-labelled cysteine residue was built with Crystallographic Object-Oriented Toolkit (Coot) with the help of JLigand [36]. The apo-enzyme model of WT-ADI was built based on the crystal structures of the *P. aeruginosa* homologue (Pa-ADI), of which both apo- and covalently-linked substrate complex were available (PDB IDs 1RXX and 2AAF, respectively) [37]. The substrate-bound complexes of WT-ADI and Pa-ADI were essentially superimposable, including the substrate, L-Arg. It was noticeable that in the apo-Pa-ADI structure, a side chain of residue 401 (Arg^{401}) occupied part of the space where the substrate bound. On substrate binding, Arg^{401} gave way to the substrate and was displaced outward towards the solvent as revealed by the arginine-bound Pa-ADI. The equivalent residue of Pa-ADI Arg^{401} was Met^{393} in WT-ADI. These two residues were almost superimposable in both substrate-bound structures (1S9R and 2AAF). This comparison allowed modelling of the active site of apo-WT-ADI, referencing both Pa-ADI structures (1RXX and 2AAF). Residues 390–394 of apo-WT-ADI was built based on residues 398 to 402 (Pa-ADI) surrounding one side of the active site, using Coot. The figures were rendered with PyMOL. The distance between the Trp^{264} side chain and the fluorescein moiety of 265Cf was defined by the midpoints between the CD2 and CE2 atoms on Trp^{264} and the O2 and C10 atoms on 265f.

3. Results

3.1. Protein expression and purification

Wild-type arginine deiminase (WT-ADI) and two corresponding mutants (44C and 265C) were expressed and purified. They were highly expressed as inclusion bodies and were purified by a single-step column with high purity (Fig. S1). High purity of WT-ADI was observed after the re-folding process (Fig. S1, lane 4). The purity of WT-ADI was further enhanced using the Q column in 20% elution buffer (Fig. S1, lane 7). The purified WT-ADI had a yield of about 16 mg/l cell, which accounted for about 88% recovery (Table S1). Its specific activity was 28.7 U/mg (Table S1). The mass of WT-ADI detected by Liquid Chromatography-Electrospray Ionization Mass Spectrometry (LC-ESI-MS) was measured as 46,377 Da (calculated mass = 46,376 Da), which had a proton attached on the protein (Fig. 1a). The two mutants were purified by the same method as WT-ADI. The specific activity of 44C and 265C was 16.0 and 19.4 U/mg, respectively (Table S1). The measured mass values of 44C (Fig. S2a) and 265C (Fig. 1b) was 463,651 and 46,362 Da, respectively.

3.2. The verification of the attachment of fluorescein-5-maleimide (F5M) on 44C and 265C

The purified 44C and 265C were labelled with F5M to become 44Cf and 265Cf, respectively. The ability to generate fluorescence of 44Cf and 265Cf was analysed by SDS-PAGE (Figs. 2 and S3). Before the labelling, 44C and 265C did not show any intrinsic fluorescence (Figs. 2 and S3). To confirm the complete labelling on them, the masses of 44Cf and 265Cf were verified by LC-ESI-MS measurements. The measured masses of 44Cf and 265Cf were 46,777 and 46,789, respectively (Figs. 1c and S2b). Their mass differences before and after labelling were exactly 427 Da (corresponding to the mass of F5M) (Fig. 1b, c,

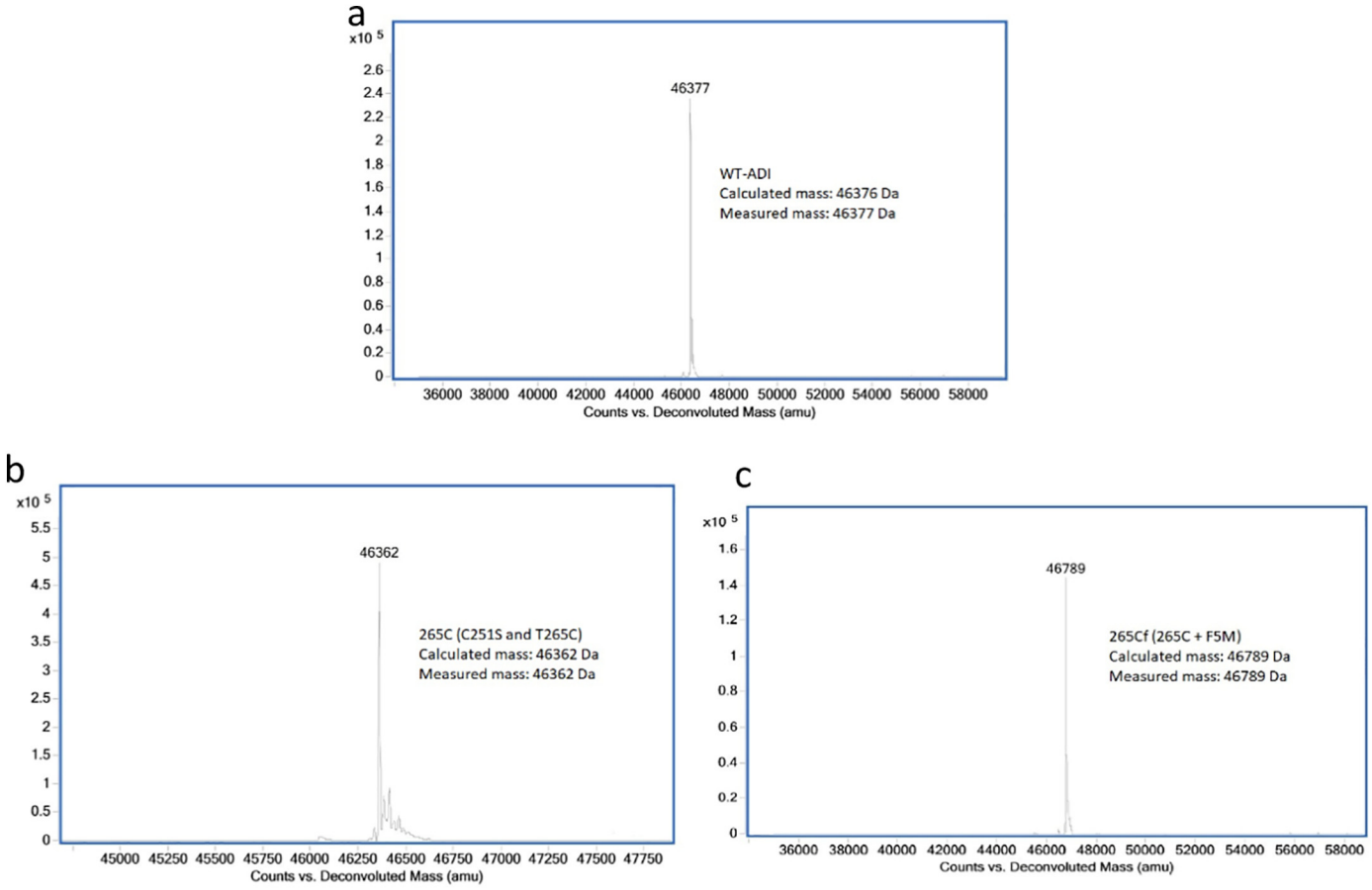

Fig. 1. ESI-MS spectra of different arginine deiminases. (a) Wild type arginine deiminase (WT-ADI). (b) 265C. (c) 265Cf.

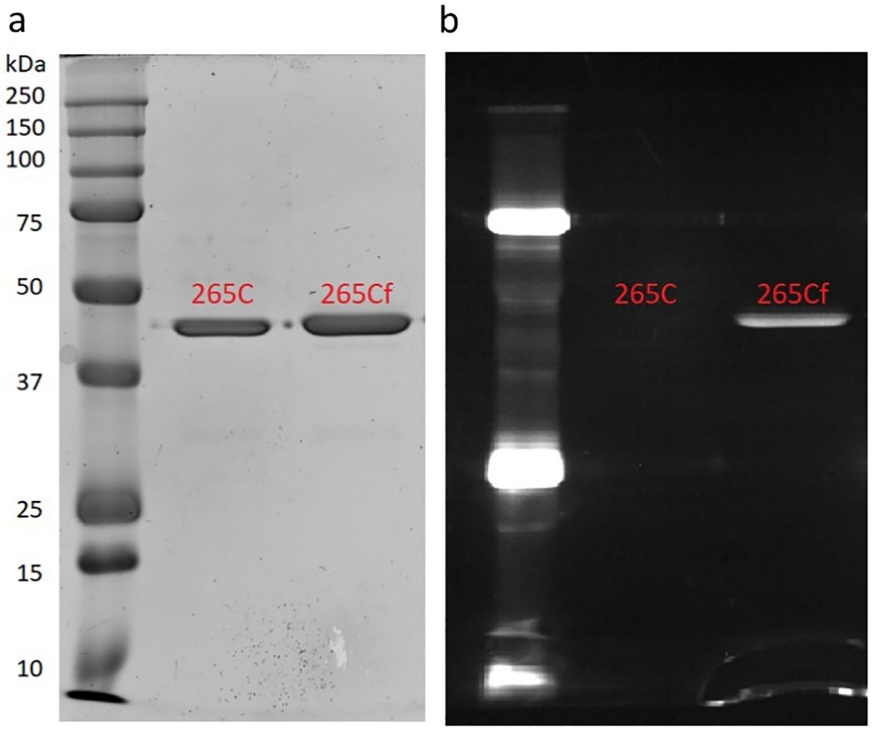

Fig. 2. SDS-PAGE analysis of 265C before and after it was labelled with fluorescin-5-maleimide. (a) Staining with Coomassie Blue. (b) Exposure under ultraviolet light.

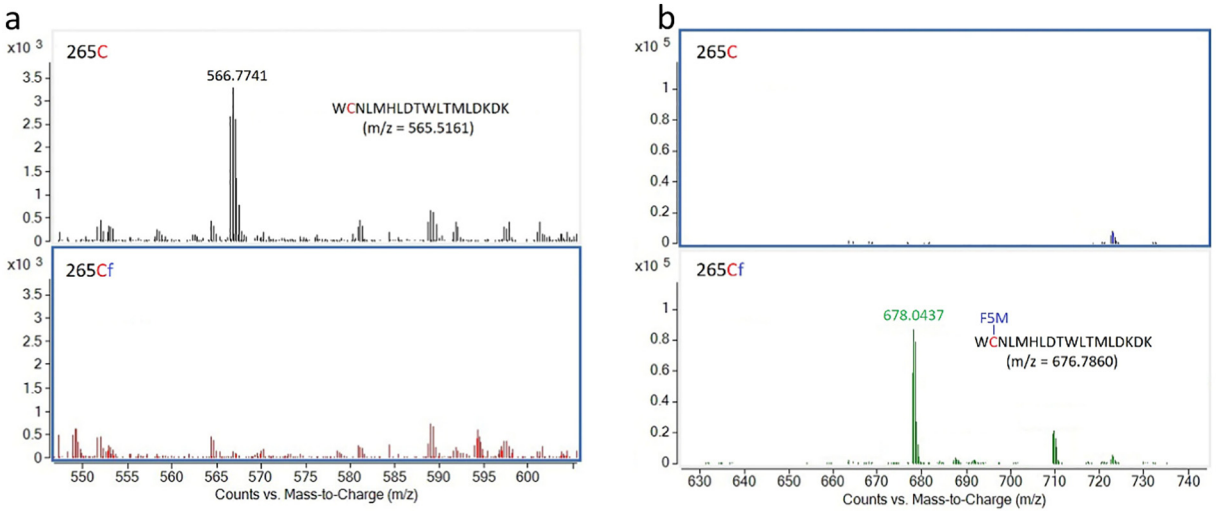

Fig. 3. ESI-MS spectra of trypsin digested 265C and 265Cf. (a) A peptide fragment showing the amino acid sequence from the position of 264 to 281 (WCNLMHLDTWLTMLDKDK) with a *m/z* value of 566.7741 present in 265C but not 265Cf (b) A peptide fragment showing the amino acid sequence from 264 to 281 (WCNLMHLDTWLTMLDKDK + fluorescein-5-maleimide (F5M) + water adduct) with a *m/z* value of 678.0437 only present in 265Cf but not in 265C.

S2a, and S2b), showing a single attachment of F5M on them. It was also found that 265C was completely labelled by F5M since a peak corresponding to the mass of 265C was absent from the spectrum of Fig. 1c. Unlike 265Cf, the peak corresponding to 44C was observed in Fig. S2b, showing its incomplete labelling by using the same method.

To ensure the site-specific attachment of F5M on designated Cys^{44} and Cys^{265}, parallel trypsin digestions were done on mutants before and after labelling. Their digested peptide fragments were analysed by LC-ESI-MS. In the analysis of 265C and 265Cf, it was found that a peptide fragment (W***C***NLMHLDTWLTMLDKDK) representing the amino acid sequence from the position of W264 to K281 with a mass to charge ratio (*m/z*) of 566.7741 was only found in 265C but not in 265Cf (Fig. 3a). On the other hand, a *m/z* value of 676.786 corresponding to the incorporation of that peptide segment and F5M was only present in 265Cf but not in 265C (Fig. 3b). These results proved the site-specific labelling of 265C by F5M. Furthermore, unspecific labelling on Cys^{398} at the active site was not observed in 265Cf since a peptide segment (VLPFHGNQLSLGMGNAR***C***MSMPLSR) representing the amino acid sequence from the position of V381 to R405 without the attachment of F5M on its cysteine residue (m/z = 906.457) could be detected in 265Cf (Fig. S4). On the other hand, the site-specific attachment o F5M on 44C was also confirmed by the presence of the peptide (LDEL***C***FSAILESHDAR) associated with F5M in the spectrum of 44Cf (Fig. S5).

3.3. The kinetic parameters of arginine deiminases

The kinetic parameters of WT-ADI and two mutants before and after labelling with F5M were studies. There kinetic profiles were shown in Figs. 4 and S6. The catalytic efficiency of WT-ADI, 265C and 44C was 988 ± 272, 1025 ± 311 and 138 ± 52 mM^{-1} s^{-1}, respectively (Table inside Figs. 4 and S6). The double mutations (Cys^{251}→Ser^{251} and Thr^{265}→Cys^{265}) introduced on ADI conserved the catalytic efficiency as wild-type while the mutations on Cys^{251}→Ser^{251} and Lys^{44}→Cys^{44} significantly lowered its catalytic efficiency, which was about a 7-fold decrease. The attachment of F5M did not alter their catalytic efficiencies (Figs. 4 and S6).

3.4. The fluorescence intensity of 44Cf and 265Cf in phosphate-buffered saline (PBS) system

44Cf and 265Cf performed as 'turn-off' biosensors when reacting with L-Arginine (L-Arg). Before the addition of L-Arg, their fluorescence remained at their baseline intensities (labelled as 0 μM L-Arg in figures) (Fig. 5a and c). After the addition of L-Arg, the fluorescence intensities were quenched and restored to the baseline intensities upon the depletion of L-Arg (Fig. 5a and c).

However, they acted differently in two ways. The first difference was the rates of restoring to the baseline intensities were varied, in which the 265Cf was faster than 44Cf (Fig. 5a and c). The second difference was the percentage changes of fluorescence intensities against the concentrations of L-Arg. It was shown that the fluorescence intensity at time = 0 decreased with respect to the increase of L-Arg concentration in 44Cf (Fig. 5a) while it remained at almost the same level when the concentration of L-Arg increased in 265Cf (Fig. 5c). When their percentages of fluorescence intensities changes were plotted against the concentration of L-Arg, it was shown that they did not have strong linear relationships (Fig. 5b and d).

It was interesting to note that the duration of fluorescence quenching changed with respect to the concentration of L-Arg in 265Cf (Fig. 6a). The higher the concentration of L-Arg was, the longer the time it would take for restoration of the fluorescence to the baseline intensity (labelled as 0 μM L-Arg in figures). Also, this quenching was specific to L-Arg but not other amino acids, including asparagine, aspartic acid, agmatine, citrulline, glutamine, and glutamic acid (Fig. 7a and b). Therefore, the time when the

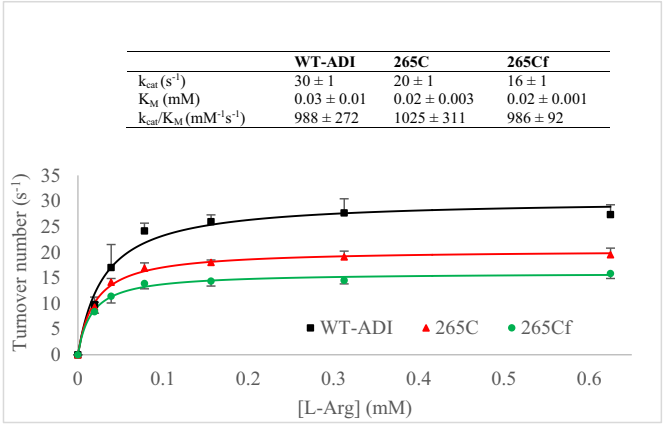

Fig. 4. The kinetic profiles of wild-type arginine deiminase (WT-ADI), 265C and 265Cf. The results were expressed as means ± S.D.

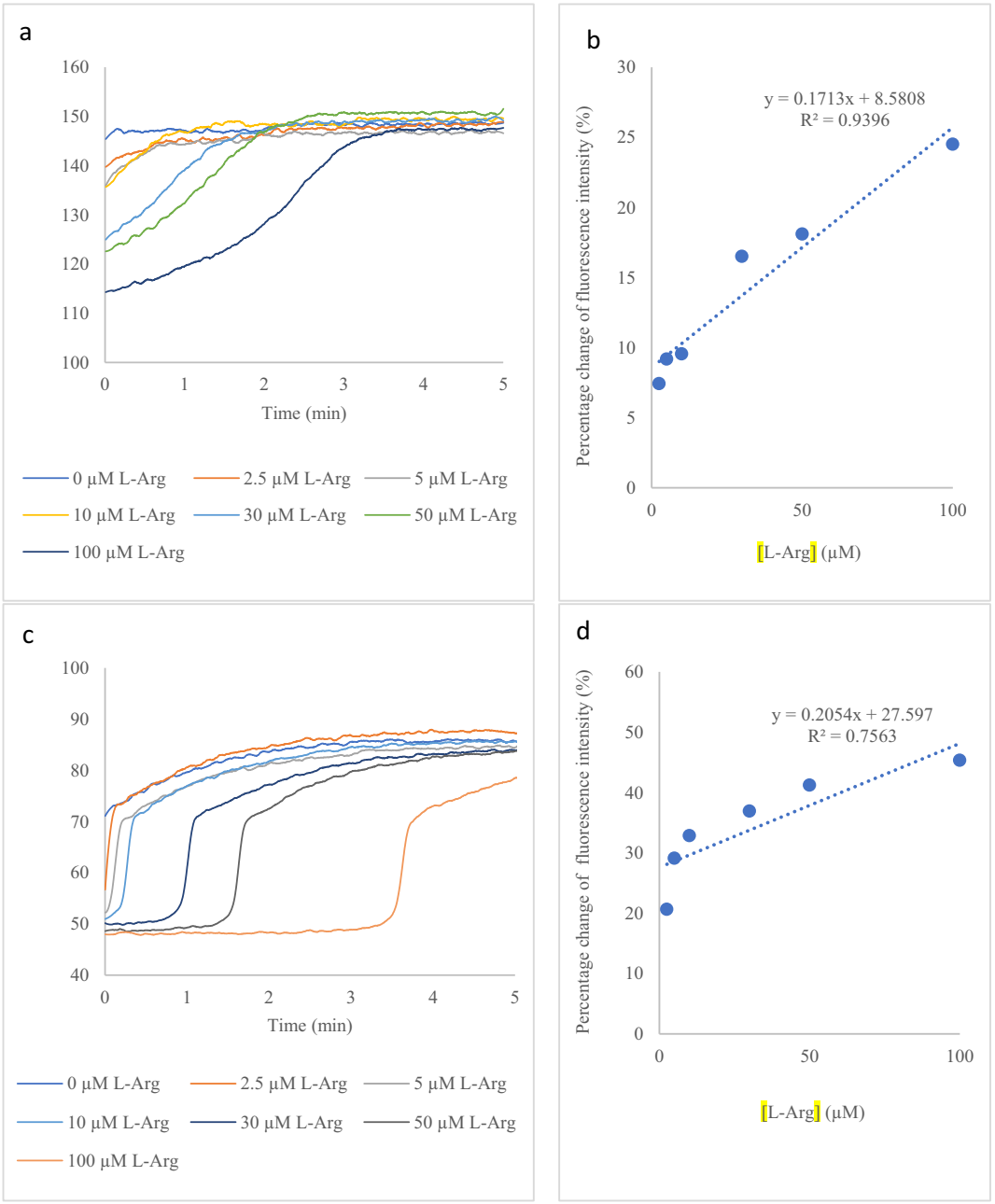

Fig. 5. Time-course fluorescence measurements on two fluorescein-labelled mutants (44Cf and 265Cf) with different concentrations of L-Arg in PBS solution. L-Arg in different concentrations (0–100 μM) was mixed with (a) 44Cf and (b) 265Cf, respectively. The relationship between the percentage changes of fluorescence intensities and L-Arg concentrations in 44Cf and 265Cf was shown in (c) and (d), respectively.

fluorescence changes occurred was used to correlate with L-Arg concentrations. The time was collected by finding the maximum rate of the fluorescence change (Fig. 6b). The relationship between the time at the maximum rate of the fluorescence change and the L-Arg concentration was linear with $R^2 = 0.9988$ (Fig. 6c). The linear detection range was 2.5–100 μM of L-Arg and the assay response time was 0.15–4 min (Fig. 6c). However, the time at the maximum rate of fluorescence change could not be well defined in 44Cf as in 265Cf (Fig. S7).

3.5. Application of 265Cf on the detection of L-Arg in fetal bovine serum

Since 265Cf showed its linear relationship with respect to the concentration of L-Arg, it was applied to the detection of L-Arg concentration in fetal bovine serum by using the standard addition method and without sample-pre-treatment. The pattern of fluorescence change in serum was similar to that in PBS system, in which the fluorescence intensity was suppressed in the presence of L-Arg and then rose back to the baseline intensity (Fig. 8a).

Although the fluorescence intensity changes were lower in serum in comparison to that in the calibration curve (Figs. 6a, 8a and S8a), the times at the maximum rate of the fluorescence change could still be defined (Figs. 8b and S8b) and were linearly proportional to L-Arg concentration (Figs. 8c and S8c). By using standard addition method, the L-Arg concentration in fetal bovine serum was measured as 47.2 ± 6.0 μM by the first batch biosensor and as 48.9 ± 1.2 μM by the second batch biosensor. These were in line with the result determined by mass spectrometry, which was 48.3 ± 1.5 μM (Table 2). This application showed the potential of 265Cf on the determination of L-Arg in complex systems, i.e. biological samples.

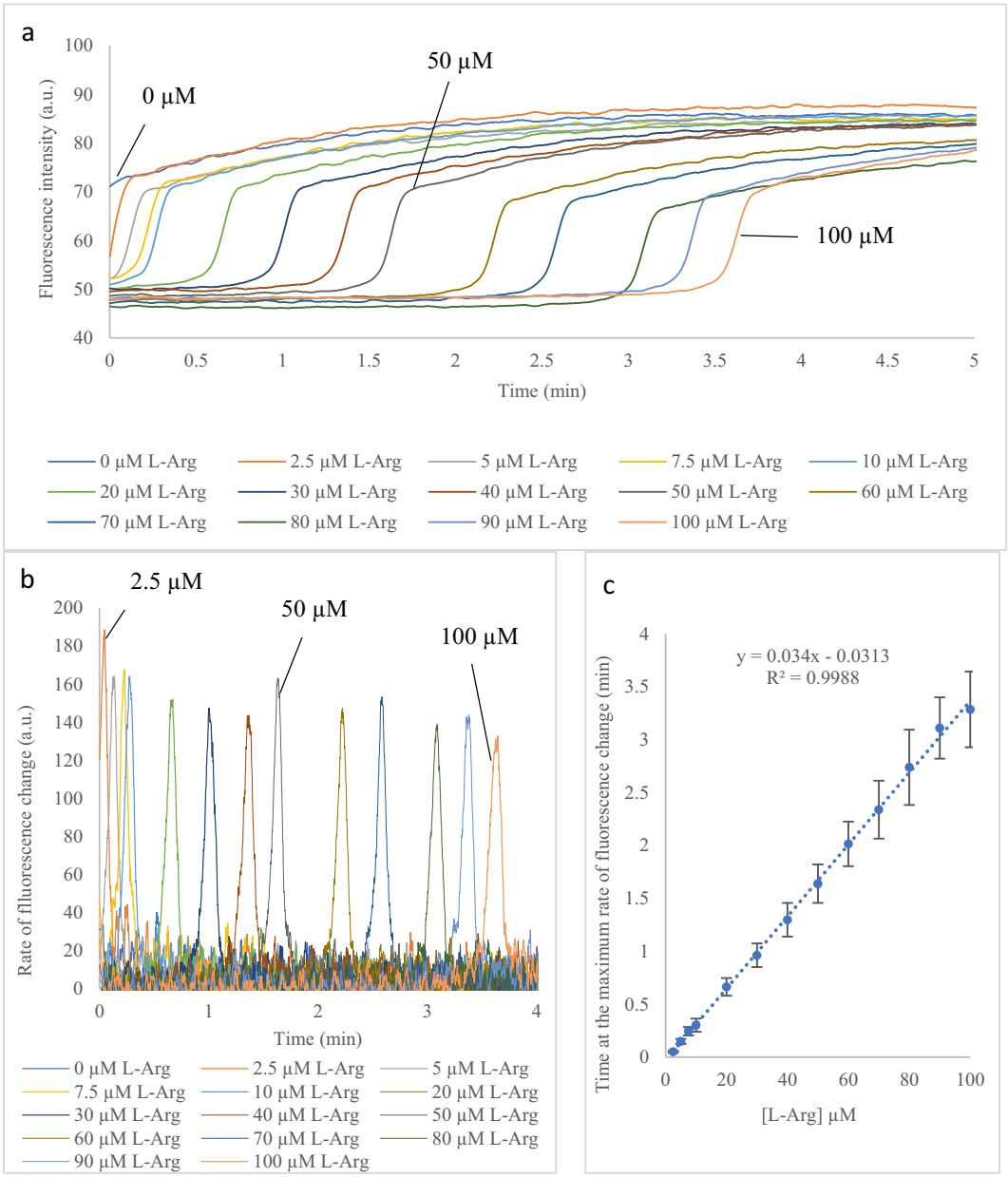

Fig. 6. Time-course fluorescence measurements on 265Cf in different concentrations of L-Arg in PBS solution. L-Arg in different concentrations (0–100 μM) was mixed with (a) 265Cf. (b) The rates of the fluorescence changes at different concentrations of L-Arg. (c) The linear relationship between the time at the maximum rate of the fluorescence change and the L-Arg concentration.

3.6. Molecular modelling of 265Cf

The phenomenon on the fluorescence intensity changes induced by 265Cf in the presence of L-Arg was investigated by molecular modelling. We hypothesized that a residue Trp^{264} adjacent to fluorescein-labelled cysteine could give rise to fluorescence quenching. To illustrate this, two models were manually built: the apo-protein (Fig. 9a) and the L-Arg-complexed protein (Fig. 9b). In the apo-protein, the fluorescein moiety (light green) on Cys^{265} was remote from Trp^{264} while residue Met^{393} occupied part of the empty active site (Fig. 9a). From our apo protein model, this distance was measured to be 10.8 Å (Fig. 9a). In the presence of L-Arg (orange), Met^{393} was pushed outward which caused the fluorescein moiety (dark green) to move closer by approximately 5 Å to Trp^{264} and its fluorescence was thus quenched (Fig. 9b). From our complexed model, this distance was now 6.0 Å (Fig. 9b).

4. Discussion

In the present study, we developed a fluorescent biosensor (265Cf) that provided an alternative method for the rapid and specific determination of L-Arginine (L-Arg). One of the main features of our biosensor is the high specificity. Existing developed L-Arg biosensors utilize immobilized enzymes, such as arginases, ureases, and arginine deiminases to generate ammonium for analysis [3,25–27]. The ability of ammonium to generate potential and pH differences renders it to become analytes [26,29,33]. However, this reduces the specificity of the biosensors since side products may be already present in samples to interfere with the detection results. For example, the presence of urea in biological samples can also be hydrolysed by ureases to produce ammonium for detection, which leads to overestimation of L-Arg concentrations [25–27]. To obtain an accurate detection of the amount of L-Arg in samples, corrections need to be done to eliminate interfering signals

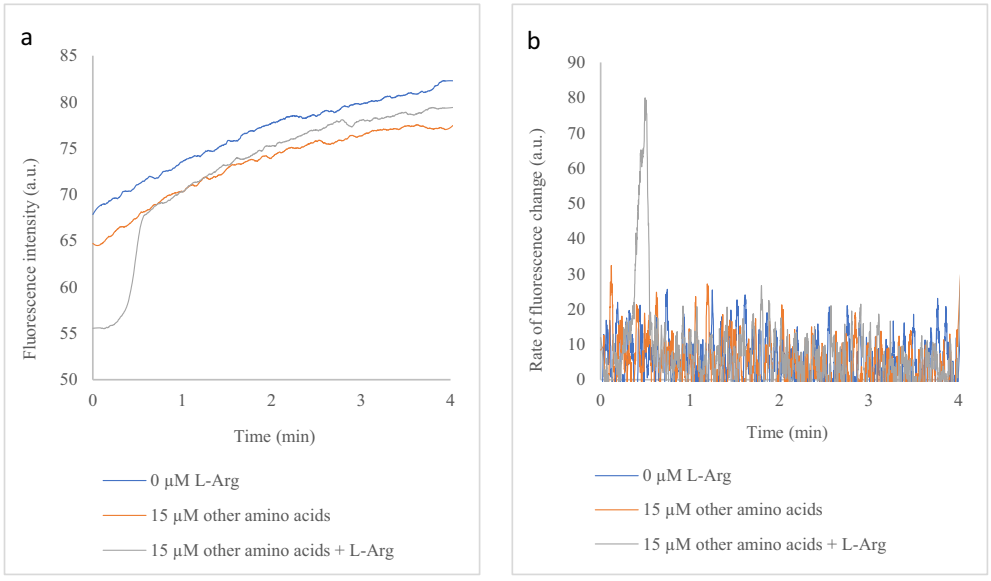

Fig. 7. Time-course fluorescence measurements on 265Cf mixed with 15 μM amino acid solution with and without the presence of L-Arg. (a) 15 μM amino acid solution, including asparagine, aspartic acid, agmatine, citrulline, glutamine and glutamic acid, with and without the presence of L-Arg. (b) The rates of the fluorescence changes of 265Cf mixed with 15 μM amino acid solutions with and without the presence of L-Arg.

[25–27]. Unlike other L-Arg biosensors, we made use of the specificity of arginine deiminase (ADI) and directly measured L-Arg by using a fluorophore attached on the enzyme. The fluorophore (fluorescein-5-malemide, F5M) sensed changes in the local environmental, which were the conformational changes of ADI upon L-Arg binding, to generate changes in fluorescence intensity for quantitative analysis. Another unique feature of our biosensor was the simplicity of the manufacturing process. To fabricate our biosensor, only two steps were required, which were the production of ADI mutant and the labelling process. The process was relatively simplified and time-efficient than the manufacturing processes of existing biosensors.

We rationally selected two sites, which were Lys^{44} on a beta-sheet and Thr^{265} on a flexible loop, to be mutated as cysteine residue on ADI. They were located at the entrance of the solvent channel, where took part in the structural conformation changes upon substrate binding [35].To avoid unspecific labelling, the intrinsic Cys^{251} present on ADI was mutated into Ser^{251}, namely C251S. Using C251S as a template, mutations on Lys^{44}→Cys^{44} and Thr^{265}→Cys^{265} were introduced to generate two mutants (44C and 265C) and these two mutants were individually site-specific labelled by F5M to become 44Cf and 265Cf. It was interesting to note that 44Cf had a 7-fold decrease in the catalytic efficiency than the wild-type (WT-ADI) while 265Cf showed a conserved catalytic efficiency (Figs. 4 and S6). On the other hand, complete labelling succeeded in 265Cf but not in 44Cf (Figs. 1c and S2b). Based on these results, 265Cf was chosen as a candidate for the detection of L-Arg concentration.

Conventional fluorescent biosensors make use of the relationship between the percentage fluorescence changes and the concentrations of analytes [38,39]. However, this relationship was only found in 44Cf, but not in 265Cf. It was observed that the fluorescence intensity increased slightly with respect to the increase in L-Arg concentration in 44Cf (Fig. 5a). In contrast to 44Cf, the fluorescence changes generated by 265Cf remained almost the same when the concentration of L-Arg increased (Fig. 5c). Neither of them showed a good linear relationship between percentage fluorescence changes and L-Arg concentrations (Fig. 5b and d).

However, in 265Cf, we discovered that the duration of fluorescence quenching was prolonged when the concentration of L-Arg increased in phosphate-buffered saline (PBS) system (Fig. 6a). This quenching was only observed in the presence of L-Arg, but not other amino acids, showing a high specificity of our biosensor (Fig. 7). It was postulated that residue Trp^{264} contributed to quench the fluorescence of the fluorescein moiety [40,41]. Results from the modelling study illustrated that Trp^{264} could act as a quencher when the fluorescein moiety moved closer towards it as a result of L-Arg occupying the active site of 265Cf (Fig. 9). With this feature, 265Cf showed a correlation between the time at its maximum rate of fluorescence change and L-Arg concentration (Fig. 6b). They were linearly proportional to each other with $R^2 = 0.9988$ (Fig. 6c). The detection range was 2.5 to 100 μM and the assay time was 0.15–4 min. Our biosensor could achieve a higher sensitivity (2.5 μM) than the existing L-Arg biosensors (Table 1).

With a high sensitivity and specificity, our biosensor, 265Cf, was attempted to be applied on biological samples (a more complicated matrix system) for the determination of L-Arg. It demonstrated a quantitative analysis of fetal bovine serum without the need of sample pre-treatment. The pattern of the resulting fluorescence changes was similar to the one measured in the PBS system, but the fluorescence intensity changes significantly reduced and the times at the maximum rate of fluorescence change shifted due to the matrix interferences (Fig. 8a and b). By using standard addition method, the L-Arg concentration in serum determined by two different batches of biosensor were 47.2 ± 6.0 and 48.9 ± 1.2 μM L-Arg, which were in good agreement with the results obtained from mass spectrometry (48.3 ± 1.5 μM) (Figs. 8c, S8c and Table 2). This showed the potential use of 265Cf on matrix-complicated systems, such as biological samples. Furthermore, this biosensor still performed a good linearity at low concentration range of L-Arg in the standard addition method, suggesting it could be a rapid clinical tool for the measurement of low L-Arg concentration in samples, such as human serum from cancer patients treated with arginine depletion drugs [13].

5. Conclusion

A fluorescent L-arginine (L-Arg) biosensor (265Cf) was developed by site-specific attachment of fluorescein-5-maldeimide (F5M) to generate fluorescence quenching, which were induced by the structural conformational changes of the bioengineered ADI as a result of L-Arg binding. A linear relationship between the time at the maximum rate of the fluorescence change and the concentrations of L-Arg was revealed. The linear detection range was 2.5–100 μM with good linearity of $R^2 = 0.9988$. The assay response

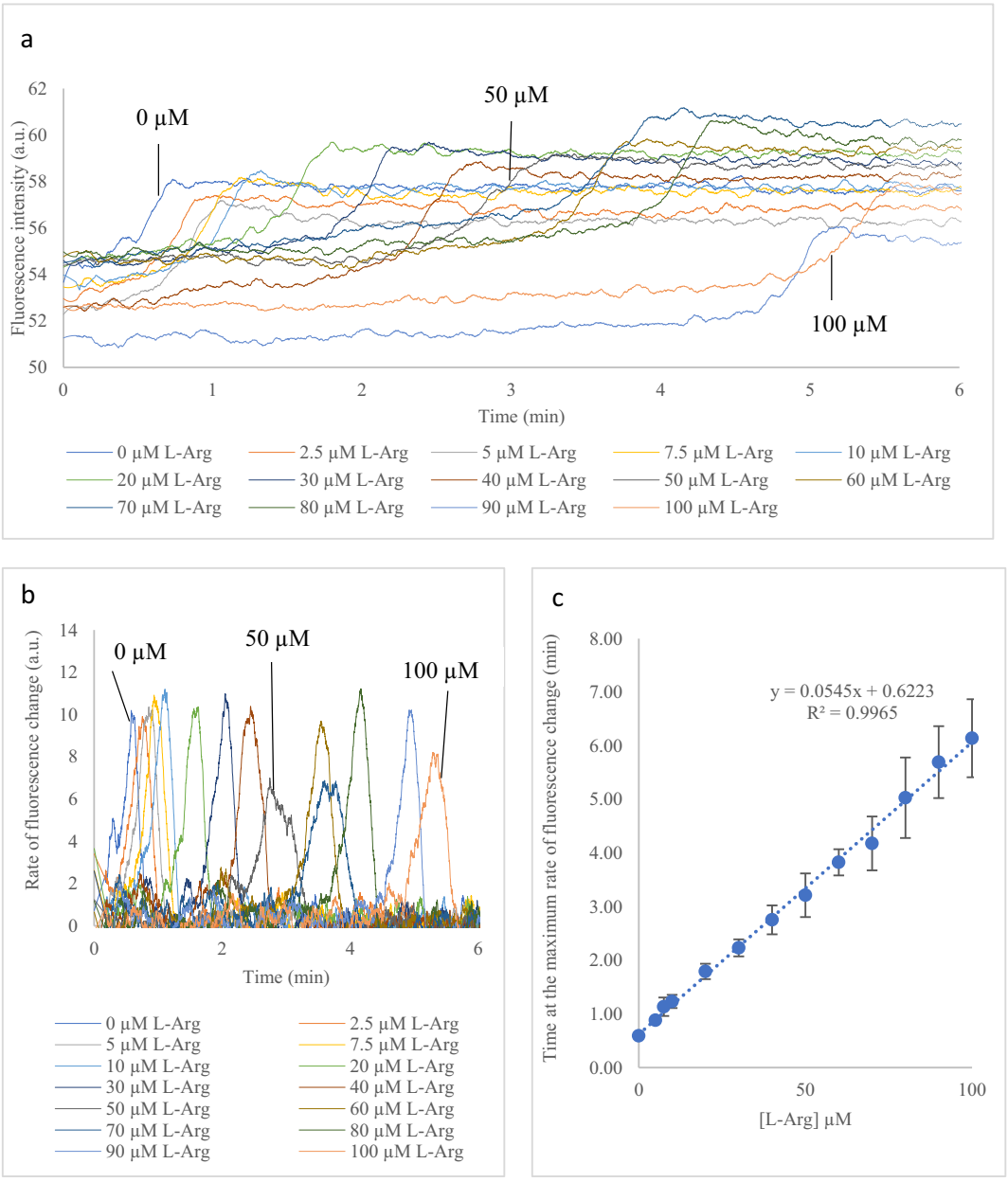

Fig. 8. Time-course fluorescence measurements on 265Cf (Batch 1) in different concentrations of L-Arg in fetal bovine serum. L-Arg in different concentrations (0–100 μM) was spiked into serum and mixed with (a) 265Cf. (b) The rates of the fluorescence changes at different concentrations of L-Arg. (c) The linear relationship between the time at the maximum rate of fluorescence change and the L-Arg concentration.

time was 0.15–4 min, which was comparable to that of the existing L-Arg biosensors. By using the standard addition method, 265Cf could be applied to the detection of L-Arg in bovine serum without any sample pre-treatment, showing its potential use on food and pharmaceutical samples. Our study demonstrated a simple strategy for making a biosensor to provide an alternative method for the rapid determination of L-Arg. This strategy is universal and provides insight on the detection of biological samples by using site-specific fluorophore-labelled enzymes.

Table 2
The L-arginine concentration in fetal bovine serum analysed by 265Cf and mass spectrometry. Each batch enzyme was performed in $n = 3$.

	L-arginine concentration (μM)
265Cf (Batch 1 in present study)	47.2 ± 6.0
265Cf (Batch 2 in present study)	48.9 ± 1.2
Mass spectrometry [42]	48.3 ± 1.5

CRediT authorship contribution statement

Suet-Ying Tam: Data Curation, Formal analysis, Investigation, Methodology, Validation, Visualization, Writing - Original Daft

Sai-Fung Chung: Data Curation, Formal analysis, Investigation, Methodology, Validation, Visualization, Writing – Review & Editing

Yu Wai Chen: Software, Writing – Review & Editing

Yik-Hing So: Investigation

Pui-Kin So: Investigation

Wing-Lam Cheong: Formal analysis, Writing – Review & Editing

Kwok-Yin Wong: Conceptualization, Funding acquisition, Supervision

Yun-Chung Leung: Conceptualization, Funding acquisition, Writing – Review & Editing, Supervision

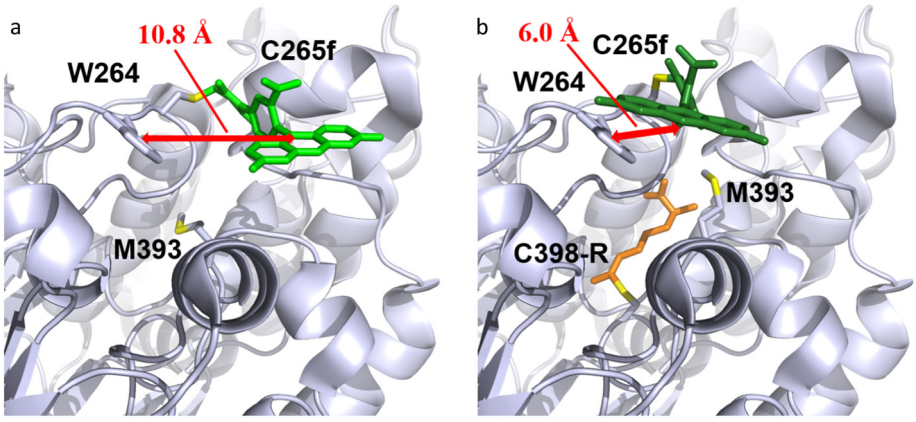

Fig. 9. Molecular models of arginine deiminase in the absence and presence of L-Arg. (a) In the apo-protein, the fluorescein moiety (light green) was remote from Trp^{264} while Met^{393} occupied part of the empty active site. The distance between the Trp^{264} side chain and the fluorescein moiety was measured as 10.8 Å. (b) When L-Arg (orange) bound to Cys^{393}, Met^{393} was pushed outward and caused the fluorescein moiety to be quenched (dark green) when it moved closer to Trp^{264}. The distance between the Trp^{264} side chain and the fluorescein moiety was measured as 6.0 Å. Sulphur atoms are in yellow.

Funding

This work was supported by University Supporting Fund (1-BBAE), Project of Strategic Importance (1-ZE18 & 1-ZE21), the Lo Ka Chung Charitable Foundation Limited (847E), Research in Chirosciences and Chemical Biology Funding Scheme (BBX8), and PolyU Strategic Development Special Project (ZVH9).

Declaration of competing interest

The authors declare that they have no conflict of interest.

Acknowledgements

We would like to thank the University Research Facility in Life Sciences (ULS) for providing instruments for doing the studies.

Appendix A. Supplementary data

Supplementary data to this article can be found online at https://doi.org/10.1016/j.ijbiomac.2020.09.134.

References

[1] D.S. Lind, Arginine and cancer, J. Nutr. 134 (10 Suppl) (2004) (2837S-2841S; discussion 2853S).
[2] S. Haghighi-Poodeh, B. Kurganov, L. Navidpour, P. Yaghmaei, A. Ebrahim-Habibi, Characterization of arginine preventive effect on heat-induced aggregation of insulin, Int. J. Biol. Macromol. 145 (2020) 1039–1048.
[3] N. Verma, A.K. Singh, M. Singh, L-arginine biosensors: a comprehensive review, Biochem. Biophys. Rep. 12 (2017) 228–239.
[4] P.N. Cheng, Y.C. Leung, W.H. Lo, S.M. Tsui, K.C. Lam, Remission of hepatocellular carcinoma with arginine depletion induced by systemic release of endogenous hepatic arginase due to transhepatic arterial embolisation, augmented by high-dose insulin: arginase as a potential drug candidate for hepatocellular carcinoma, Cancer Lett. 224 (1) (2005) 67–80.
[5] Y.L. Vissers, C.H. Dejong, Y.C. Luiking, K.C. Fearon, M.F. von Meyenfeldt, N.E. Deutz, Plasma arginine concentrations are reduced in cancer patients: evidence for arginine deficiency? Am. J. Clin. Nutr. 81 (5) (2005) 1142–1146.
[6] L. Hu, Y. Gao, Y. Cao, Y. Zhang, M. Xu, Y. Wang, Y. Jing, S. Guo, F. Jing, X. Hu, Z. Zhu, Association of plasma arginine with breast cancer molecular subtypes in women of Liaoning province, IUBMB Life 68 (12) (2016) 980–984.
[7] L.C. Burrage, Q. Sun, S.H. Elsea, M.M. Jiang, S.C. Nagamani, A.E. Frankel, E. Stone, S.E. Alters, D.E. Johnson, S.W. Rowlinson, G. Georgiou, C. Members of Urea Cycle Disorders, B.H. Lee, Human recombinant arginase enzyme reduces plasma arginine in mouse models of arginase deficiency, Hum. Mol. Genet. 24 (22) (2015) 6417–6427.
[8] W.T. Shen, X.Y. Zhang, X. Fu, J.J. Fan, J.Y. Luan, Z.L. Cao, P. Yang, Z.Y. Xu, D.W. Ju, A novel and promising therapeutic approach for NSCLC: recombinant human arginase alone or combined with autophagy inhibitor, Cell Death Dis. (2017) 8.
[9] S. Xu, S.K. Lam, P.N. Cheng, J.C. Ho, Recombinant human arginase induces apoptosis through oxidative stress and cell cycle arrest in small cell lung cancer, Cancer Sci. 109 (11) (2018) 3471–3482.
[10] S.M. Tsui, W.M. Lam, T.L. Lam, H.C. Chong, P.K. So, S.Y. Kwok, S. Arnold, P.N. Cheng, D.N. Wheatley, W.H. Lo, Y.C. Leung, Pegylated derivatives of recombinant human arginase (rhArg1) for sustained in vivo activity in cancer therapy: preparation, characterization and analysis of their pharmacodynamics in vivo and in vitro and action upon hepatocellular carcinoma cell (HCC), Cancer Cell Int. 9 (2009) 9.
[11] P.E. Hall, R. Lewis, N. Syed, R. Shaffer, J. Evanson, S. Ellis, M. Williams, X.X. Feng, A. Johnston, J.A. Thomson, F.P. Harris, R. Jena, T. Matys, S. Jefferies, K. Smith, B.W. Wu, J.S. Bomalaski, T. Crook, K. O'Neill, D. Paraskevopoulos, R.S. Khadeir, M. Sheaff, S. Pacey, P.N. Plowman, P.W. Szlosarek, A phase I study of pegylated arginine deiminase (Pegargiminase), cisplatin, and pemetrexed in argininosuccinate synthetase 1-deficient recurrent high-grade glioma, Clin. Cancer Res. 25 (9) (2019) 2708–2716.
[12] A.K. Singh, R. Sharma, M. Singh, N. Verma, Electrochemical determination of L-arginine in leukemic blood samples based on a polyaniline-multiwalled carbon nanotube-magnetite nanocomposite film modified glassy carbon electrode, Instrum. Sci. Technol. 48 (4) (2020) 400–416.
[13] E. Beddowes, J. Spicer, P.Y. Chan, R. Khadeir, J.G. Corbacho, D. Repana, J.P. Steele, P. Schmid, T. Szyszko, G. Cook, M. Diaz, X.X. Feng, A. Johnston, J. Thomson, M. Sheaff, B.W. Wu, J. Bomalaski, S. Pacey, P.W. Szlosarek, Phase 1 dose-escalation study of pegylated arginine deiminase, cisplatin, and pemetrexed in patients with argininosuccinate synthetase 1-deficient thoracic cancers, J. Clin. Oncol. 35 (16) (2017) (1778-+).
[14] S.F. Chung, C.F. Kim, S.Y. Tam, M.C. Choi, P.K. So, K.Y. Wong, Y.C. Leung, W.H. Lo, A bioengineered arginine-depleting enzyme as a long-lasting therapeutic agent against cancer, Appl. Microbiol. Biotechnol. 104 (9) (2020) 3921–3934.
[15] S.F. Chung, C.F. Kim, S.Y. Kwok, S.Y. Tam, Y.W. Chen, H.C. Chong, S.L. Leung, P.K. So, K.Y. Wong, Y.C. Leung, W.H. Lo, Mono-PEGylation of a thermostable arginine-depleting enzyme for the treatment of lung cancer, Int. J. Mol. Sci. 21 (12) (2020).
[16] C.A. Uthurry, J.A.S. Lepe, J. Lombardero, J.R.G. Del Hierro, Ethyl carbamate production induced by selected yeasts and lactic acid bacteria in red wine (vol 94, pg 262-270, 2006), Food Chem. 105 (2) (2007) 666.
[17] D.W. Lachenmeier, M.C. Lima, I.C. Nobrega, J.A. Pereira, F. Kerr-Correa, F. Kanteres, J. Rehm, Cancer risk assessment of ethyl carbamate in alcoholic beverages from Brazil with special consideration to the spirits cachaca and tiquira, BMC Cancer 10 (2010) 266.
[18] C.S. Ough, D. Stevens, T. Sendovski, Z. Huang, D. An, Factors contributing to urea formation in commercially fermented wines, Am. J. Enol. Vitic. 41 (1) (1990) 68–73.
[19] S. Kodama, T. Suzuki, S. Fujinawa, P. Delateja, F. Yotsuzuka, Urea contribution to ethyl carbamate formation in commercial wines during storage, Am. J. Enol. Vitic. 45 (1) (1994) 17–24.
[20] R. Ridwan, H.R.A. Razak, M.I. Adenan, W.M.M. Saad, Development of isocratic RP-HPLC method for separation and quantification of L-citrulline and L-arginine in watermelons, Int. J. Anal. Chem. 2018 (2018).
[21] M.G. Fleszar, J. Wisniewski, M. Krzystek-Korpacka, B. Misiak, D. Frydecka, J. Piechowicz, K. Lorenc-Kukula, A. Gamian, Quantitative analysis of L-arginine, dimethylated arginine derivatives, L-citrulline, and dimethylamine in human serum using liquid chromatography-mass spectrometric method, Chromatographia 81 (6) (2018) 911–921.
[22] X. Lai, J.A. Kline, M. Wang, Development, validation, and comparison of four methods to simultaneously quantify l-arginine, citrulline, and ornithine in human plasma using hydrophilic interaction liquid chromatography and electrospray tandem mass spectrometry, J. Chromatogr. B Anal. Technol. Biomed. Life Sci. 1005 (2015) 47–55.
[23] S. Vigneshvar, C.C. Sudhakumari, B. Senthilkumaran, H. Prakash, Recent advances in biosensor technology for potential applications - an overview, Front. Bioeng. Biotechnol. 4 (2016) 11.

[24] P. Teena, K. Jagjit, K. Raman, K. Kumar, Development of electrochemical biosensor for detection of asparagine in leukemic samples, Int. J. Pharm. Sci. Res. 7 (2) (2016) 783–788.
[25] M.T. Zhybak, L.Y. Fayura, Y.R. Boretsky, M.V. Gonchar, A.A. Sibirny, E. Dempsey, A.P.F. Turner, Y.I. Korpan, Amperometric L-arginine biosensor based on a novel recombinant arginine deiminase, Microchim. Acta 184 (8) (2017) 2679–2686.
[26] S. Karacaoglu, S. Timur, A. Telefoncu, Arginine selective biosensor based on arginase-urease immobilized in gelatin, Artif. Cell Blood Sub. 31 (3) (2003) 357–363.
[27] N.E. Stasyuk, G.Z. Gaida, M.V. Gonchar, L-arginine assay with the use of arginase I, Appl. Biochem. Microbiol. 49 (5) (2013) 529–534.
[28] D.M. Ivnitskii, J. Rishpon, Biosensor based on direct-detection of membrane-potential induced by immobilized hydrolytic enzymes, Anal. Chim. Acta 282 (3) (1993) 517–525.
[29] O.Y. Saiapina, S.V. Dzyadevych, N. Jaffrezic-Renault, O.P. Soldatkin, Development and optimization of a novel conductometric bi-enzyme biosensor for L-arginine determination, Talanta 92 (2012) 58–64.
[30] N. Stasyuk, O. Smutok, G. Gayda, B. Vus, Y. Koval'chuk, M. Gonchar, Bi-enzyme L-arginine-selective amperometric biosensor based on ammonium-sensing polyaniline-modified electrode, Biosens. Bioelectron. 37 (1) (2012) 46–52.
[31] K. An, H.D. Duong, J.I. Rhee, Ratiometric fluorescent L-arginine and L-asparagine biosensors based on the oxazine 170 perchlorate-ethyl cellulose membrane, Eng. Life Sci. 17 (8) (2017) 847–856.
[32] O.V. Soldatkina, O.O. Soldatkin, T.P. Velychko, V.O. Prilipko, M.A. Kuibida, S.V. Dzyadevych, Conductometric biosensor for arginine determination in pharmaceutics, Bioelectrochemistry 124 (2018) 40–46.
[33] N.Y. Stasyuk, G.Z. Gayda, M.V. Gonchar, L-arginine-selective microbial amperometric sensor based on recombinant yeast cells over-producing human liver arginase I, Sensors Actuators B Chem. 204 (2014) 515–521.
[34] M. Knipp, M. Vasak, A colorimetric 96-well microtiter plate assay for the determination of enzymatically formed citrulline, Anal. Biochem. 286 (2) (2000) 257–264.
[35] K. Das, G.H. Butler, V. Kwiatkowski, A.D. Clark Jr., P. Yadav, E. Arnold, Crystal structures of arginine deiminase with covalent reaction intermediates; implications for catalytic mechanism, Structure 12 (4) (2004) 657–667.
[36] P. Emsley, K. Cowtan, Coot: model-building tools for molecular graphics, Acta Crystallogr. D Biol. Crystallogr. 60 (Pt 12 Pt 1) (2004) 2126–2132.
[37] A. Galkin, L. Kulakova, E. Sarikaya, K. Lim, A. Howard, O. Herzberg, Structural insight into arginine degradation by arginine deiminase, an antibacterial and parasite drug target, J. Biol. Chem. 279 (14) (2004) 14001–14008.
[38] W.L. Cheong, M.S. Tsang, P.K. So, W.H. Chung, Y.C. Leung, P.H. Chan, Fluorescent TEM-1 beta-lactamase with wild-type activity as a rapid drug sensor for in vitro drug screening, Biosci. Rep. 34 (2014) (523-+).
[39] P.H. Chan, P.K. So, D.L. Ma, Y. Zhao, T.S. Lai, W.H. Chung, K.C. Chan, K.F. Yiu, H.W. Chan, F.M. Siu, C.W. Tsang, Y.C. Leung, K.Y. Wong, Fluorophore-labeled beta-lactamase as a biosensor for beta-lactam antibiotics: a study of the biosensing process, J. Am. Chem. Soc. 130 (20) (2008) 6351–6361.
[40] S.E. Mansoor, M.A. Dewitt, D.L. Farrens, Distance mapping in proteins using fluorescence spectroscopy: the tryptophan-induced quenching (TrIQ) method, Biochemistry 49 (45) (2010) 9722–9731.
[41] M. Moller, A. Denicola, Protein tryptophan accessibility studied by fluorescence quenching, Biochem. Mol. Biol. Educ. 30 (3) (2002) 175–178.
[42] H. Prinsen, B.G.M. Schiebergen-Bronkhorst, M.W. Roeleveld, J.J.M. Jans, M.G.M. de Sain-van der Velden, G. Visser, P.M. van Hasselt, N.M. Verhoeven-Duif, Rapid quantification of underivatized amino acids in plasma by hydrophilic interaction liquid chromatography (HILIC) coupled with tandem mass-spectrometry, J. Inherit. Metab. Dis. 39 (5) (2016) 651–660.